EPSC Abstracts
Vol. 11, EPSC2017-286-1, 2017
European Planetary Science Congress 2017

The Orbit Planes of Impactors that Formed Elongated Martian Craters

E. Sefton-Nash (1), Z. Faes (1), O. Witasse (1) and B. Buchenburger (2).
(1) ESTEC, European Space Agency, The Netherlands, (2) KU Leuven, Belgium. (e.sefton-nash@cosmos.esa.int)

Abstract

Elongated craters can form from low angle impacts. The distinguishing morphological properties of elongated craters and their ejecta become more pronounced with decreasing impact angle, which allows ease of identification of craters formed by grazing impacts. Using remote sensing data and an ellipse-fitting algorithm, we update a pre-existing database of elongated craters on Mars [1, 2, 3] to better characterize selected properties regarding crater shape, location and estimated age. We use the retrieved impact direction to constrain the possible orbit planes that impactors may have originated from.

1. Database update

Our updated database comprises a GIS project registered to MOLA topography, THEMIS IR mosaics and relevant high-resolution visible images from HRSC, CTX and HiRISE. Shapefiles include preliminary estimates of crater geometric properties (centre position, size, eccentricity, azimuth, etc…).

2. Retrieving best-fit geometric parameters

To retrieve best-fit values of geometric parameters, we fit ellipses to crater rim crests (Fig. 1, upper). Idealized elongated crater rims are not necessarily ellipses, but this approach provides a numerically consistent way of retrieving crater geometry. We assess the goodness of fit, D, between crater rims and ellipses of given sizes and orientations. D is computed as the sum of the cartesian distance between all pairs of closest vertices in the model ellipse and the polygon that traces the crater rim crest. Provided that crater rims are sufficiently well-resolved, an unconstrained non-linear multivariate optimization (Nelder-Mead simplex direct search [4]) is then used to refine initial parameters (a_0,b_0,x_0,y_0,α_0) (Fig. 1, lower) to minimize D and retrieve the corresponding size and orientation parameters. To reduce influence on D of spatial distortion introduced by the map projection, distances are calculated in a local equirectangular projection with the point of true scale at the feature centroid.

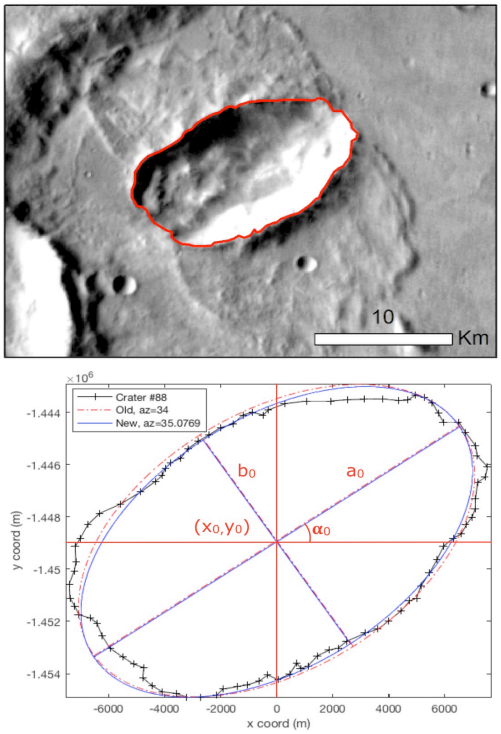

Figure 1: Upper – Example of mapped crater rim. Lower – Initial and best fit ellipse parameters for an elongated crater at 40.98°E, 24.46°S.

Oblique impacts form craters with morphology that can be used to ascribe the sense of the impact. For systematic assessment of features in our database, we identify several criteria whose cumulative indication of the same impact direction allow ascription of sense for the impactors trajectory. Asymmetric crater shapes could indicate that greater excavation energy was imparted to the surface at the point of first impact. The shape and distribution of ejecta is also

telling: In highly oblique cases, a butterfly pattern is present. In other cases ejecta distribution indicates greater deposition on one side, with a paucity forming a V-shaped zone of exclusion, opposite to the impact direction. Craters resulting from a body travelling in the prograde direction constitute ~50% of all craters in the database, while those in retrograde direction constitute ~35%. The remainder have undetermined impact directions.

3. Age

Impact chronology-derived ages from [5] show that most elongated craters on surfaces aged 3.7 to 4.1 Ga were formed by bodies travelling in a prograde direction. This presents an upper age limit for crater formation, but unit ages are consistent with the period in which Phobos and Deimos are hypothesized to have originated from a debris disk formed from a giant impact [6, 7].

4. Inclination of orbit planes

The inclination of the parent orbit plane for each elongated crater is calculated using the best-fit azimuth and crater latitude. The azimuth for a given elongated crater is interpreted to coincide with the ground-projection of the orbit from which it originated, represented as a great circle at an inclination, *i*. For a fixed rotation axis, the azimuth (measured counter-clockwise from East) and latitude of mapped craters is a function of only the orbit inclination. The relationship is independent of longitude and the position of the ascending node. We plot the azimuth, latitude and corresponding orbit inclination for selected features (Fig. 2 – upper). We exclude craters whose state of degradation or geomorphology warranted further investigation before azimuth and sense can be meaningfully retrieved, leaving 191 features from an initial 248.

5. Discussion

The distribution of orbit inclination with respect to Mars' present-day rotation axis indicates a relative paucity of impactors originating from low inclination orbits (Fig. 2 – lower). Thus, no low-angle impactors originated from Mars' present equatorial plane.

Moonlets in a debris disk with unstable, decaying orbits would impact Mars at a shallow angle [6, 7]. To investigate the decaying moonlet hypothesis, true polar wander of Mars' rotation axis [8, 9] is expected to be the predominant factor, because while obliquity cycles would indeed modify the relationship between latitude, azimuth and orbit plane inclination, a transient debris disk that lingered for several Ma would be expected to align with Mars' equator throughout obliquity variations. Further analysis will identify any groups of craters formed under the same orbit planes and rotation pole.

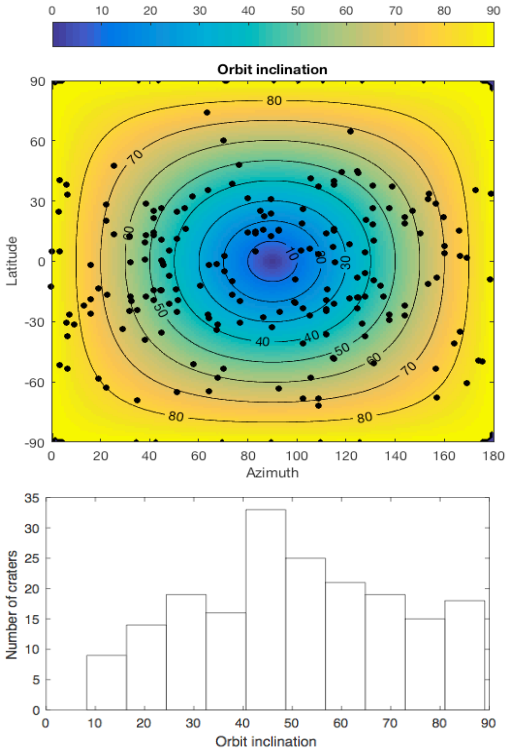

Figure 2: Upper – Distribution of best-fit elongated crater azimuths and latitude, and the retrieved orbit plane inclination, *i*, for Mars' current rotation axis. Lower – Distribution of *i* for 191 elongated craters.

References

[1] Schultz and Lutz-Garihan (1982) J. Geophys. Res. 87, (S01) p. A84–A96. **[2]** Bottke, W. F. et al (2000) *Icarus* 145, p. 108—121. **[3]** Buchenberger, B. (2011) *EPSC-DPS Joint Meeting 2011*, p. 738. **[4]** Lagarias, J. C. et al. (1998), *SIAM J. Optimization* 9 (1), p. 112-147. **[5]** Tanaka, K.L et al (2014) Geologic map of Mars: U.S. Geological Survey Scientific Investigations Map 3292. **[6]** Rosenblatt, P. et al (2016) *Nature Geoscience* 9, p. 581-583. **[7]** Craddock, R. A. (2011) *Icarus* 211(2), p. 1150-1161. **[8]** Schultz and Lutz (1988), *Icarus* 73, p. 91-141. **[9]** Bouley, S. et al. (2016), *Nature* 531, p. 344-347.